



ISSN: 0067-2904

## Preparation and Characterization of TiO<sub>2</sub> Nanoparticles With and Without Magnetic Field Effect Via Hydrothermal Technique

Howraa Ghassan Hameed\*, Nadia A. Abdulrahman

Department of Chemistry, College of Science, University of Baghdad, Baghdad, Iraq

Received: 29/6/2022

Accepted: 19/10/2022

Published: 30/7/2023

### ABSTRACT

With and without the use of magnetic fields, titanium dioxide (TiO<sub>2</sub>) nanoparticles were synthesized using the hydrothermal method at extremely high temperatures and pressures. Titanium tetra isopropoxide [Ti(C<sub>12</sub>H<sub>28</sub>O<sub>4</sub>)] was used for the preparation, which was performed at pH 7 and under temperatures of 160 and 190 °C. UV spectroscopy, XRD crystallography, FE-SEM microscopy were used for characterizations. From UV spectroscopy, the energy gap values were clearly affected by the increase in temperature and the presence of the magnetic field. At the temperatures of 160 and 190 °C for TiO<sub>2</sub> without magnetic field, FE-SEM microscopy images have shown an average crystal diameter of 13.436 and 12.551 nm, respectively. While for TiO<sub>2</sub> with the presence of magnetic field, the crystal diameters were found to be 14.665 and 14.468 nanometers, respectively, at same temperatures. Additionally, XRD analysis has revealed that the average crystal size of TiO<sub>2</sub> at 160 and 190 °C without a magnetic field is 13.13 and 11.59 nanometers, respectively. While the crystal sizes for TiO<sub>2</sub> in the presence of a magnetic field were determined to be 13.19 and 12.93 nanometers, respectively.

**Keywords:** TiO<sub>2</sub> nanoparticles, Hydrothermal method, Magnetic field, Nanoscience, Nanotechnologies, Semiconductors.

## تحضير وتوصيف جسيمات TiO<sub>2</sub> النانوية مع وبدون تأثير المجال المغناطيسي عن طريق التقنية الحرارية المائية

حوراء غسان حميد\* ، نادية عبد الكريم عبد الرحمن

قسم الكيمياء، كلية العلوم، جامعة بغداد، بغداد، العراق

### الخلاصة

تم التحضير الجسيمات لثاني اوكسيد التيتانيوم مع وبدون المجال المغناطيسي عن طريق التقنية الحرارية المائية تحت درجة حرارة عالية وضغط مرتفع. تم اجراء التحضير باستخدام التيتانيوم رباعي الأيزوبروبوكسايد عند الرقم الهيدروجيني 7 وعند درجات حرارة 160 و 190 درجة مئوية. تم استخدام التحليل الطيفي للأشعة فوق البنفسجية، حيود الأشعة السينية، المجهر الالكتروني الماسح للتوصيفات. من التحليل الطيفي للأشعة فوق البنفسجية وجد ان قيم فجوة الطاقة تأثرت بشكل واضح بزيادة درجة الحرارة ووجود المجال المغناطيسي. عند درجات حرارة 160 و 190 درجة مئوية لثاني اوكسيد التيتانيوم بدون مجال مغناطيسي، اظهر الفحص المجهرية متوسط اقطار بلورية تبلغ 13.436 و 12.551 نانومتر، على التوالي. بينما بالنسبة لثاني اوكسيد التيتانيوم مع

\*Email: [howraa.ghassan89@gmail.com](mailto:howraa.ghassan89@gmail.com)

وجود مجال مغناطيسي، وجد اقطار البلورات كانت 14.665 و 14.468 نانومتر، على التوالي، في نفس درجات الحرارة. ايضا عند درجات حرارة 160 و 190 درجة مئوية لثاني اوكسيد التيتانيوم بدون مجال مغناطيسي، اظهرت قياسات XRD متوسط سمك بلوري يبلغ 13.13 و 11.59 نانومتر، على التوالي. بينما بالنسبة لثاني اوكسيد التيتانيوم مع وجود مجال مغناطيسي، وجد ان سمك البلورة 13.19 و 12.93 نانومتر على التوالي.

## 1. Introduction

Nanotechnology is the design, manufacture, and use of structures, devices, and systems at the nanoscale in order to produce something new or different [1]. Nanoscience is the study of structures and materials on the ultra-scales of nanometers with an average diameter of 100 nm. These tools may be used to determine the structure, form, materials, and measurements. These instruments, which were designed to characterize objects as tiny as a few nanometers, include the Atomic Force Microscope (AFM), Scanning Tunneling Microscope (STM), Scanning Electron Microscope (SEM), Transmission Electron Microscope (TEM), and X-Ray Diffraction (XRD) [2-4]. Additionally, it has certain features as a result of the numerous techniques utilized to prepare these minerals, such as hydrothermal technology. One of the most popular processes for producing nanomaterials at high temperatures and pressures is hydrothermal synthesis [5]. High-crystallized powders with narrow particle size distribution, high purity, and process conditions such solute concentration and ease of large-scale production are some of the benefits of the hydrothermal synthesis approach [6-9]. Anatase (tetragonal), brookite (orthorhombic), rutile (tetragonal), and  $\text{TiO}_2$  B (monoclinic) are the four natural phases of titanium dioxide ( $\text{TiO}_2$ ), which is a semiconductor material [10]. Aside from that, its band gap values for the brookite (2.96 eV), rutile (3.02 eV), and anatase (3.2 eV) phases [11, 12]. Because the catalysis at this size has the biggest surface area, anatase is the most common form of  $\text{TiO}_2$  that exists as a crystal [13]. In a magnet or one of the sources that generates a magnetic field, the distribution of magnetic force is referred to as the magnetic field [14].  $\text{TiO}_2$  NPs are used for wide range of applications, such as catalysis, white pigment for paints, cosmetics, food colorants, pharmaceuticals, biomedical fields, sensors, biosensors, solar cells, dye sensitized solar cell, microelectronics, electrochemistry, and charge spreading devices [15]. Numerous techniques have been used to study the production of ultrafine titanium dioxide nanoparticles, including hydrothermal, solvothermal, chemical co-precipitation, chemical vapor deposition (CVD), sol-gel technique, sputtering, hydrolysis, and micro emulsion approach [16].

## 2. Experimental

Using a hydrothermal technique, titanium dioxide nanoparticles with and without magnetic fields have been synthesized. 50 mL of a 0.1 M TTIP [ $\text{Ti}(\text{C}_{12}\text{H}_{28}\text{O}_4)$ ] solution (M.W = 58.11  $\text{g}\cdot\text{mol}^{-1}$ , Biuret = 80%, BDH) was gradually added to 5 M KOH (M.W = 284.2  $\text{g}\cdot\text{mol}^{-1}$ , purity = 97%, ALDRICH) in order to achieve the pH level up to 7. The solution was placed inside a Teflon (type PPL) lined stainless steel autoclave hydrothermal system (type PTFE) after 30 minutes of stirring. This was accomplished under high temperature and high-pressure conditions. In order to maintain the heat sustained at 160 and 190 °C for 5 hours, the autoclave was totally closed. In order to generate  $\text{TiO}_2$  nanoparticles under the influence of a magnetic field, two magnetic bars were placed inside two basins, each of which contained 5 liters of 25 °C water. A magnetic field with a 325 Tesla power was being used. The subsequent separation of the solution was centrifuged for 10 to 15 minutes at a speed of 5000 rpm to separate it. The precipitate was five times rinsed with 100 mL of distilled water before being dried for 20 hours at 100 °C in the oven. The powder was then treated to a 2-hour process of calcination at 450 °C. All samples were kept in storage until analysis.

## 3. Results and Discussions

### 3.1. UV-Vis measurements

UV-Vis measurements provided a rough understanding of the optical and photoelectric characteristics, as well as information on the particle size and energy gap values of these materials. The values of the energy gap were computed using Einstein's equation:  $E = h\nu = hc/\lambda$ , where  $E$  = band gap energy,  $h$  = Planck constant =  $6.63 \times 10^{-34}$  Js,  $\nu$  = frequency of photon,  $c$  = speed of light in a vacuum =  $3 \times 10^8$  m/s,  $\lambda$  = Wavelength of photon [17].

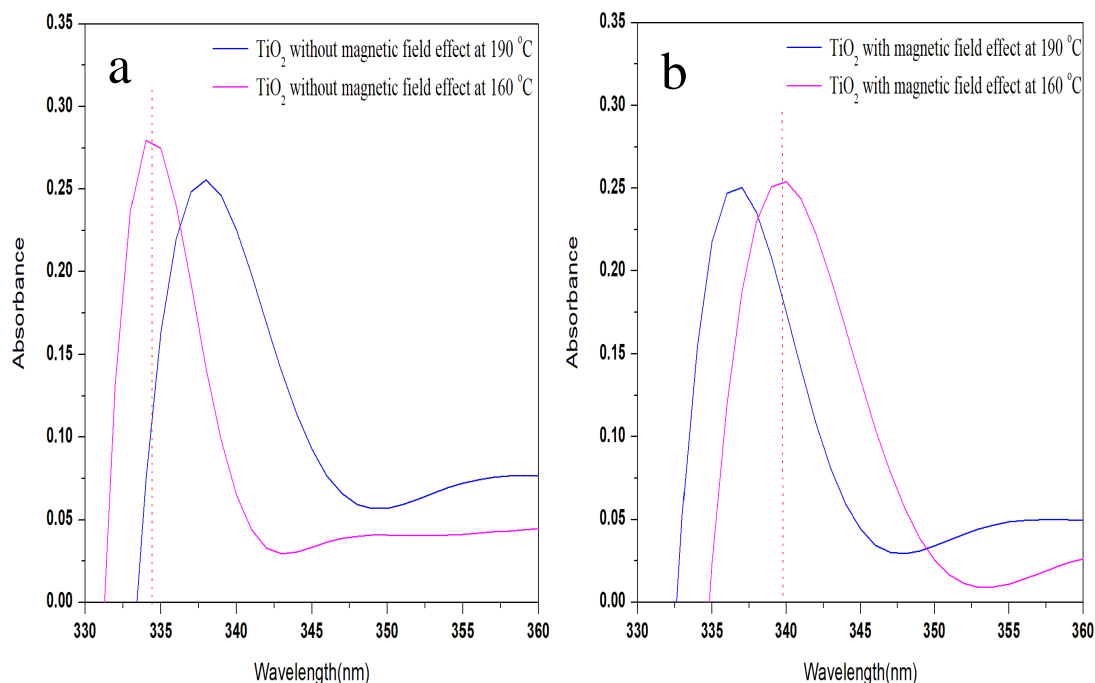


**Figure 1:** Comparison of UV spectra for. (a) for TiO<sub>2</sub> nanoparticles without magnetic field effect at 160 and 190 °C. (b) for TiO<sub>2</sub> with magnetic field effect at 160 and 190 °C

**Table 1:** Energy gap values for TiO<sub>2</sub> nanoparticles manufactured with and without magnetic field influence at 160 and 190 °C were obtained using the Einstein equation.

Materials	Temperature (°C)	Wavelength (nm)	energy gap (eV)
TiO <sub>2</sub> without magnetic field effect	160	335	3.70
<u>TiO<sub>2</sub> with magnetic field effect</u>		<u>337</u>	<u>3.68</u>
TiO <sub>2</sub> without magnetic field effect	190	338	3.67
<u>TiO<sub>2</sub> with magnetic field effect</u>		<u>342</u>	<u>3.63</u>

The magnetic field effect causes the absorbance of TiO<sub>2</sub> nanoparticles to decrease between 160 and 190 °C. This indicates that the magnetic field's impact grows as TiO<sub>2</sub> temperature rises, as seen in Figure 1. As a result, at the same temperatures, the magnetic field impact caused  $\lambda_{max}$  to slightly increase. As a result, the energy gap for TiO<sub>2</sub> nanoparticles without the influence of a magnetic field was 3.70 and 3.67 eV, respectively, at 160 and 190 °C. For TiO<sub>2</sub> with magnetic field effect at the same temperature, 3.68 and 3.63 eV, respectively. According to Table 1. We observed a little reduction in the energy gap values when a magnetic field was present while the temperature of the TiO<sub>2</sub> was constant. Therefore, we draw the conclusion that the influence of the magnetic field is dependent on the rise in temperatures, the development of pressure, and the crystal structure of the substance.

### 3.2. XRD Crystallography

The most significant facts concerning crystals, which were revealed by XRD crystallography, were their size and shape as well as any potential structural aberrations. Figure 2 depicts the XRD pattern of TiO<sub>2</sub> with and without the magnetic field influence that resulted from the anatase type. The intensity was slightly altered by raising the temperature to 160 and 190 °C. The peaks and angles have slightly changed positions due to the rise in temperature. The diffraction intensity at 190 °C clearly decreased in the presence of the magnetic field of 325 Tesla. Crystals' dimensions changed as a result of these shifts in angle position and peak diffraction. They can have diverse photoelectric and optical characteristics because temperature and magnetic field are important factors in improving crystal shape uniformity and lowering manufacturing flaws. We observed new peaks at 160 and 190 °C (shown by green arrows) which were not present in TiO<sub>2</sub> without the magnetic field effect; indicating that they are titanium-related. Table 2 demonstrates that at 160 and 190 °C, the presence of the magnetic field effect causes the size of crystals (D) to rise [18]. And this is due to the metallurgical nature of the semiconductor TiO<sub>2</sub>, as well as the effect of different temperature.

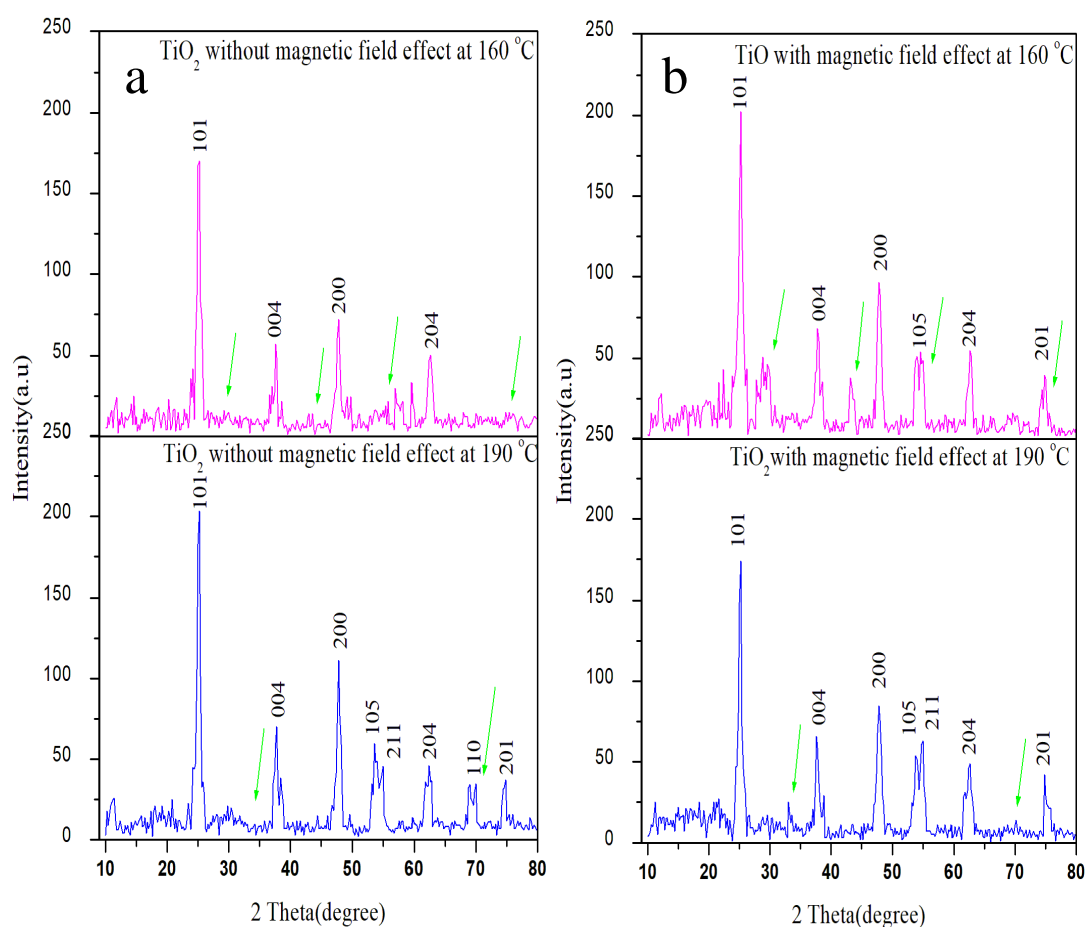


**Figure 2:** XRD crystallography, (a) for TiO<sub>2</sub> nanoparticles with magnetic field effect at 160 and 190 °C, and (b) for TiO<sub>2</sub> without magnetic field effect at same temperatures. JCPDS card no. 21-1272.

**Table 2:** The change in crystal sizes (calculated via Scherrer equation for all Miller Coefficients) as temperatures increase for TiO<sub>2</sub> with and without the magnetic field effect.

Materials	Temperature (°C)	Average of D (nm)
-----------	------------------	-------------------

TiO <sub>2</sub> without magnetic field effect	160	13.13
TiO <sub>2</sub> with magnetic field effect		13.19
TiO <sub>2</sub> without magnetic field effect	190	11.59
TiO <sub>2</sub> with magnetic field effect		12.93

### 3.3. Field Emission Scanning Electron Microscopes (FE-SEM)

In addition to providing us with a picture that allows us to understand the three dimensions of nanoparticles, FE-SEM microscopy also provides us with a general concept of the form and size of nanoparticles. At two distinct sizes of 100 nm and 1  $\mu$ m, Figure 3 displays FE-SEM images of TiO<sub>2</sub> nanoparticles without the magnetic field effect at 160 and 190 °C. According to Table 3, the average diameter was determined to be 12.551 nm at 190 °C and 13.436 nm at 160 °C. Hence, the sizes of the nanoparticles of TiO<sub>2</sub> nanoparticles at 190 °C are smaller than the sizes of nanoparticles at 160 °C. That means as long as there is an increase in temperatures there will be a decrease in the sizes of the nanoparticles. This led to growth TiO<sub>2</sub>, also affects the crystal's shape.

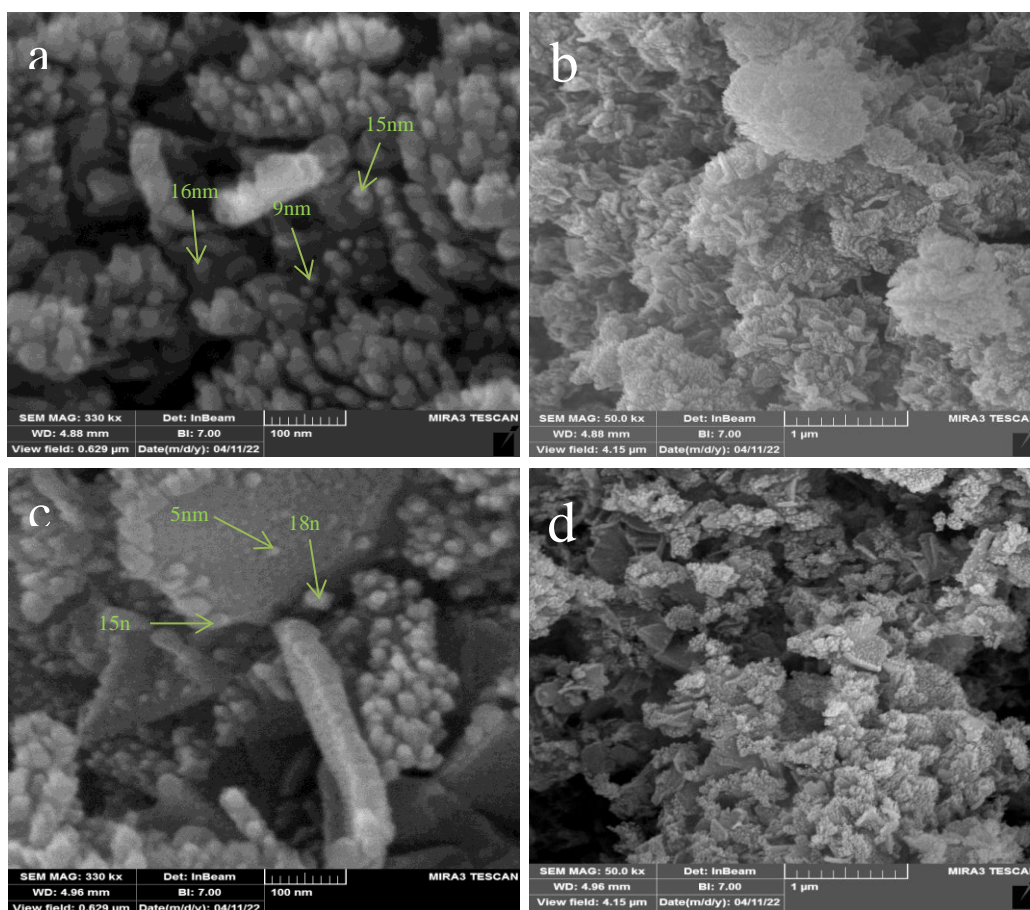


**Figure 3:** FE-SEM images for TiO<sub>2</sub> without magnetic field. a and b at 160 °C. c and d at 190 °C.

Figure 4 shows FE-SEM images of TiO<sub>2</sub> nanoparticles under magnetic effect at 160 and 190 °C at two different scales of 100 nm and 1  $\mu$ m. According to Table 3, the average diameter was determined to be 14.665 nm at 160 °C and 14.468 nm at 190 °C. As a result, at 190 °C, the diameters of the TiO<sub>2</sub> nanoparticles under the magnetic field effect are lower than those at 160

°C [4]. The crystal size of TiO<sub>2</sub> nanoparticles will typically grow when the magnetic field effect is present.

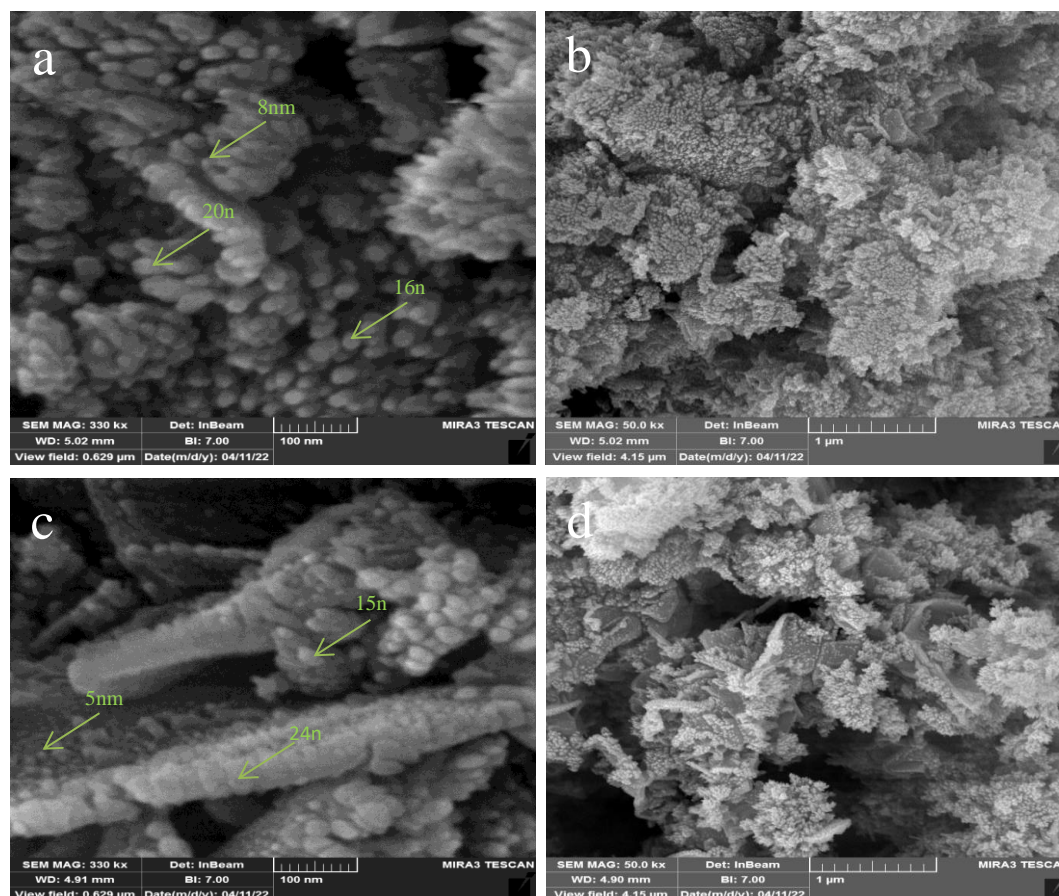


**Figure 4:** FE-SEM images for TiO<sub>2</sub> with magnetic field. a and b at 160 °C. c and d at 190 °C.

**Table 3:** Table shows the dimensions of TiO<sub>2</sub> nanoparticle with and without the magnetic field effect measured from FE-SEM images.

Materials	Temperature (°C)	Average Diameter (nm)
TiO <sub>2</sub> without magnetic field effect	160	13.436
TiO <sub>2</sub> with magnetic field effect		14.665
TiO <sub>2</sub> without magnetic field effect	190	12.551
TiO <sub>2</sub> <u>with</u> magnetic field effect		14.468

## Conclusion

It was determined that the energy gap values are affected by temperature rises and the presence of a magnetic field. The size of the crystals and the form of the nanoparticles were discovered to be clearly affected by the magnetic field's presence, temperature, pressure, and the duration of production. Because it relies on their uses, we cannot confidently state one sample is more significant than the other.

## References

- [1] C. P. Poole Jr and F. J. Owens, *Introduction to nanotechnology*. John Wiley & Sons, 2003.
- [2] R. A. Caruso and M. Antonietti, "Sol– gel nanocoating: an approach to the preparation of structured materials," *Chemistry of materials*, vol. 13, no. 10, pp. 3272-3282, 2001.

- [3] D. Grosso *et al.*, "Fundamentals of mesostructuring through evaporation-induced self-assembly," *Advanced Functional Materials*, vol. 14, no. 4, pp. 309-322, 2004.
- [4] D. Grosso *et al.*, "Highly porous TiO<sub>2</sub> anatase optical thin films with cubic mesostructure stabilized at 700 C," *Chemistry of Materials*, vol. 15, no. 24, pp. 4562-4570, 2003.
- [5] K. Byrappa and M. Yoshimura, *Handbook of hydrothermal technology*. William Andrew, 2012.
- [6] A. Abdulrahman and H. Mohammed, "Temperature and Solvent Impact on Zinc Oxide Nanostructures Synthesized via Hydro-Solvo-Thermal Technique," *International Journal of Science and Research (IJSR)*, vol. 6, no. 11, pp. 1132-1136, 2017.
- [7] N. A. Abdulrahman and N. I. Haddad, "Braggs, Scherre, Williamson–Hall and SSP analyses to estimate the variation of crystallites sizes and lattice constants for ZnO nanoparticles synthesized at different temperatures," *NeuroQuantology*, vol. 18, no. 1, p. 53, 2020.
- [8] S. T. Abdulredha and N. A. Abdulrahman, "Cu-ZnO Nanostructures Synthesis and Characterization," *Iraqi Journal of Science*, vol. 62, no. 3, pp. 708-717, 2021.
- [9] M. H. Al-Hakeem, N. A. Abdulrahman, and A. A. Alsammaraie, "Preparation and characterization of Co doped ZnO nanoparticles," *Solid State Technology*, vol. 63, pp. 636-644, 2020.
- [10] Z. F. Yin, L. Wu, H. G. Yang, and Y. H. Su, "Recent progress in biomedical applications of titanium dioxide," *Physical chemistry chemical physics*, vol. 15, no. 14, pp. 4844-4858, 2013.
- [11] S. Mahalakshmi and P. Vijaya, "Evaluation of In-vitro Biocompatibility and Antimicrobial activities of Titanium Dioxide (TiO<sub>2</sub>) Nanoparticles by Hydrothermal Method," *Nano Biomed. Eng.*, vol. 13, no. 1, pp. 36-43, 2021.
- [12] S. D. Al-Algawi, R. T. R. Rasheed, and Z. R. Rhoomi, "Structural and Optical Properties of Annealed TiO<sub>2</sub> Powder Synthesized by Hydrothermal Method," *Iraqi Journal of Science*, vol. 58, no. 3C, pp. 1683-1693, 2017.
- [13] L. Sang, Y. Zhao, and C. Burda, "TiO<sub>2</sub> nanoparticles as functional building blocks," *Chemical reviews*, vol. 114, no. 19, pp. 9283-9318, 2014.
- [14] M. M. Rahman, J.-Z. Wang, X.-L. Deng, Y. Li, and H.-K. Liu, "Hydrothermal synthesis of nanostructured Co<sub>3</sub>O<sub>4</sub> materials under pulsed magnetic field and with an aging technique, and their electrochemical performance as anode for lithium-ion battery," *Electrochimica Acta*, vol. 55, no. 2, pp. 504-510, 2009.
- [15] V. Dusastre, *Materials for sustainable energy: a collection of peer-reviewed research and review articles from Nature Publishing Group*. World Scientific, 2010.
- [16] M. Hudlikar, S. Joglekar, M. Dhaygude, and K. Kodam, "Green synthesis of TiO<sub>2</sub> nanoparticles by using aqueous extract of *Jatropha curcas* L. latex," *Materials Letters*, vol. 75, pp. 196-199, 2012.
- [17] X.-Y. Wu, X.-J. Liu, Y.-H. Wu, Q.-C. Wang, Y. Wang, and L.-X. Chi, "Quantum wave equation of photon," *International Journal of Theoretical Physics*, vol. 49, no. 1, pp. 194-200, 2010.
- [18] T. Gupta, J. Cho, and J. Prakash, "Hydrothermal synthesis of TiO<sub>2</sub> nanorods: formation chemistry, growth mechanism, and tailoring of surface properties for photocatalytic activities," *Materials Today Chemistry*, vol. 20, p. 100428, 2021.